

Enhanced critical temperature, pairing fluctuation effects, and BCS-BEC crossover in a two-band Fermi gas

Hiroyuki Tajima,¹ Yuriy Yerin,² Andrea Perali,³ and Pierbiagio Pieri^{2,4}

¹*Quantum Hadron Physics Laboratory, RIKEN Nishina Center, Wako, Saitama, 351-0198, Japan*

²*School of Science and Technology, Physics Division,
Università di Camerino, 62032 Camerino (MC), Italy*

³*School of Pharmacy, Physics Unit, Università di Camerino, 62032 Camerino (MC), Italy*

⁴*INFN, Sezione di Perugia, 06123 Perugia (PG), Italy*

(Dated: February 18, 2019)

We study the superfluid critical temperature in a two-band attractive Fermi system with strong pairing fluctuations associated with both interband and intraband couplings. We focus specifically on a configuration where the intraband coupling is varied from weak to strong in a shallow band coupled to a weakly-interacting deeper band. The whole crossover from the Bardeen-Cooper-Schrieffer (BCS) condensation of largely overlapping Cooper pairs to the Bose-Einstein condensation (BEC) of tightly bound molecules is covered by our analysis, which is based on the extension of the Nozières-Schmitt-Rink (NSR) approach to a two-band system. In comparison with the single-band case, we find a strong enhancement of the critical temperature, a significant reduction of the preformed pair region where pseudogap effects are expected, and the entanglement of two kinds of composite bosons in the strong-coupling BEC regime.

PACS numbers: 03.75.Ss, 74.20.-z, 74.25.-q

Introduction – After the realization of the BCS-BEC crossover phenomenon in ultracold Fermi gases^{1–3}, which provided a unified understanding of both weak coupling BCS Fermi superfluidity and Bose-Einstein condensation of molecular bosons^{4–12}, multi-condensates can be regarded as the next paradigmatic systems to be explored. Owing to the emergence of additional degrees of freedom of the order parameter, these multi-condensate systems can lead to the formation of a plethora of novel quantum phenomena, which are not realized in their conventional single-band counterparts. While even the single-component fermionic condensate has bridged various research fields such as nuclear physics^{12–19} and different kinds of solid-state systems^{4,7,8,20–26,28–31}, the more generic concept of multi-component BCS-BEC crossover not only builds up an interdisciplinary cross-link among strongly correlated systems but also opens a new frontier to explore the optimal configuration for high- T_c superconductivity^{32,33}.

Among the variety of unconventional superconductors recently discovered, iron-based superconducting compounds are of particular interest due to their multiband electron structure with interband couplings producing complex order parameter symmetry and multiple energy gaps. This gives new opportunities to observe experimentally the BCS-BEC crossover in a new class of superconducting materials^{26–29,31,34–36}. Thus, iron-based superconductors provide a new platform to study the electronic properties and collective phenomena in the BCS-BEC crossover regime. Current experimental activity in this direction raises fundamentally new problems about crossover and fluctuation phenomena in these superconducting compounds, which go beyond the single-band physics. Nanostructured superconductors are another promising class of materials in which the multiband

BCS-BEC crossover, in the presence of shape resonance effects, can play a key role in the control and enhancement of superconductivity^{37,38}. A multi-band structure with a small Fermi surface pocket has an important role to achieve such strongly correlated crossover regime in all these electron systems^{39–42}.

A two-band Fermi system with Josephson-type interband coupling⁴³ is also under current experimental investigation in ultracold ¹⁷³Yb atomic Fermi gases near an orbital Feshbach resonance^{44–46}. By applying an external magnetic field, the energy difference between two channels (corresponding to the band gap) can be arbitrarily tuned, and the emergence of the BCS-BEC crossover has been theoretically predicted^{47–52}. In this case, however, the situation is complicated by the simultaneous presence of shallow and deep bound states^{49,52}, and it is hard to make contact with the physical setup of multi-band superconductors.

In this paper, we address the effects of strong pairing fluctuations on the superfluid critical temperature for a two-band system with varying intra- and interband couplings. We focus in particular on the physically relevant configuration with a shallow “hot” band (in which the intraband coupling is varied from weak to strong) coupled with a deep “cold” band (with weak intraband coupling). For increasing hot-band coupling, we reveal a strong amplification of the critical temperature in comparison with the single-band case, with the interband coupling assisting such amplification, but not being crucial for its occurrence. In addition, in the intermediate (crossover) region between the BCS and BEC limits, the comparison between the superfluid critical temperature and the mean-field pair-breaking temperature shows a significant shrinking of the preformed-pair region induced by a weak interband coupling, implying a possible reduction of the

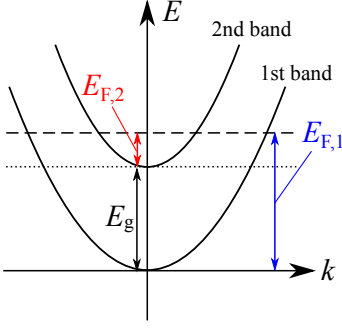


FIG. 1: The band structure considered in this work. The vertical and horizontal axes are the single-particle energy and momentum, respectively; E_g is the band gap between 1st ($i = 1$) and 2nd ($i = 2$) bands; $E_{F,i}$ indicates the Fermi energy of i -band fermions in the absence of interactions.

pseudogap effects, in lines with recent experimental findings for the FeSe multiband superconductors⁵³. Finally, in the BEC regime with finite interband coupling, an interesting coherently coupled binary mixture of composite bosons is found.

Model – For the sake of generality, we consider the following minimal model Hamiltonian^{54,55} for a three-dimensional two-band Fermi system

$$H = \sum_{\mathbf{k}, \sigma, i} \xi_{\mathbf{k}, i} c_{\mathbf{k}, \sigma, i}^\dagger c_{\mathbf{k}, \sigma, i} + \sum_{i, j} U_{ij} \sum_{\mathbf{q}} b_{\mathbf{q}, i}^\dagger b_{\mathbf{q}, j}. \quad (1)$$

Here, $c_{\mathbf{k}, \sigma, i}$ is the annihilation operator of a fermion with spin $\sigma = \uparrow, \downarrow$ and band index $i = 1, 2$, $b_{\mathbf{q}, i}^\dagger = \sum_{\mathbf{k}}^{k_0} c_{\mathbf{k}+\mathbf{q}/2, \uparrow, i}^\dagger c_{-\mathbf{k}+\mathbf{q}/2, \downarrow, i}^\dagger$ is the pair-creation operator in the i -band (where k_0 is a momentum cutoff), while $\xi_{\mathbf{k}, 1} = k^2/2m - \mu$, $\xi_{\mathbf{k}, 2} = k^2/2m + E_g - \mu$ are the kinetic energies measured from the chemical potential μ and m is the particle (effective) mass (which is assumed to be identical in the two bands). We set k_B, \hbar , and the system volume V equal to one. Fig. 1 summarizes graphically the two-band configuration we consider.

We express the intraband coupling $U_{ii} (< 0)$ in terms of the intraband scattering length a_{ii} ^{54,55}, which is given by

$$\frac{m}{4\pi a_{ii}} = \frac{1}{U_{ii}} + \sum_{\mathbf{k}}^{k_0} \frac{m}{k^2}. \quad (2)$$

The momentum cutoff k_0 is considered to be much larger than the average interparticle distance, corresponding to a short-range condition on the interaction. Specifically, we take $k_0 = 100k_{F,t}$, where $k_{F,t} = (3\pi^2 n)^{1/3}$ is the Fermi momentum defined by the total number density n , which is kept fixed. It is useful to introduce also the band Fermi momenta $k_{F,i} = (3\pi^2 n_i)^{1/3}$, defined in terms of the band densities n_1^0 and n_2^0 in the absence of interaction and at zero temperature, with the corresponding Fermi energies $E_{F,i} = k_{F,i}^2/2m$. We choose the

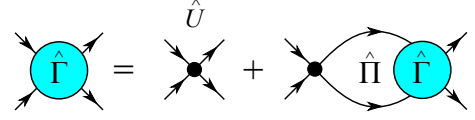


FIG. 2: Diagrammatic representation of many-body T -matrix $\hat{\Gamma}$. \hat{U} and $\hat{\Pi}$ are the 2×2 matrices of coupling constants and pair susceptibilities, respectively.

relatively large band gap $E_g = 0.75E_{F,1} = 3E_{F,2}$, which implies $k_{F,1} = (8/9)^{1/3} k_{F,t}$ and $k_{F,2} = (1/9)^{1/3} k_{F,t}$. We focus on the situation in which the shallow hot band ($i = 2$) undergoes the BCS-BEC crossover, whereas the intraband coupling in the deep cold band ($i = 1$) remains weak. In our configuration, this is achieved by taking $U_{22} = 1.1U_{11}$, which gives $(k_{F,1}a_{11})^{-1}$ ranging between $\simeq -8$ and $\simeq -4$ when we change $(k_{F,2}a_{22})^{-1}$ from the weak coupling (BCS) to the strong-coupling (BEC) regime. [We recall that for a single-band system the BCS-BEC crossover is driven by the dimensionless parameter $(k_F a)^{-1}$, which ranges from $(k_F a)^{-1} \lesssim -1$ in the weak-coupling (BCS) regime to $(k_F a)^{-1} \gtrsim 1$ in the strong-coupling (BEC) regime.]

The interband couplings are equal and real (guaranteeing the hermiticity of the Hamiltonian). For convenience, we introduce the dimensionless interband coupling \tilde{U}_{12} by setting $U_{12} = \tilde{U}_{12}(k_{F,t}/k_0)^2 E_{F,t}/n$, with $E_{F,t} = k_{F,t}^2/2m$. In this way, when \tilde{U}_{12} ranges from 0 to 5, the effects of the interband coupling on the quantities of interest will turn to vary from weak to strong. [Note that, in terms of the critical value of the intraband interaction $-U_{cr} = -2\pi^2/mk_0$ at which the scattering length a_{ii} diverges in (2), one has $U_{12}/U_{cr} = \tilde{U}_{12}(3/4)(k_{F,t}/k_0)$.]

Formalism – The NSR formalism has been widely used for studying the BCS-BEC crossover in a single-band system and was extended to a two-band system in⁵⁵. Here we adopt this formalism to calculate the effect of pairing fluctuations on the critical temperature in our system. The sum of ladder diagrams defines the many-body T -matrix $\hat{\Gamma}$, as represented in Fig. 2, which satisfies

$$\hat{\Gamma}(\mathbf{q}, i\nu_l) = [1 + \hat{U}\hat{\Pi}(\mathbf{q}, i\nu_l)]^{-1}\hat{U}, \quad (3)$$

with

$$\hat{U} = \begin{pmatrix} U_{11} & U_{12} \\ U_{21} & U_{22} \end{pmatrix}, \quad (4)$$

and

$$\hat{\Pi}(\mathbf{q}, i\nu_l) = \begin{pmatrix} \Pi_{11}(\mathbf{q}, i\nu_l) & 0 \\ 0 & \Pi_{22}(\mathbf{q}, i\nu_l) \end{pmatrix}, \quad (5)$$

where $\nu_l = 2l\pi T$ (l integer) is a boson Matsubara frequency and

$$\Pi_{ii}(\mathbf{q}, i\nu_l) = T \sum_{\mathbf{k}, i\omega_j}^{k_0} G_i^0(\mathbf{k} + \mathbf{q}, i\omega_s + i\nu_l) G_i^0(-\mathbf{k}, -i\omega_s). \quad (6)$$

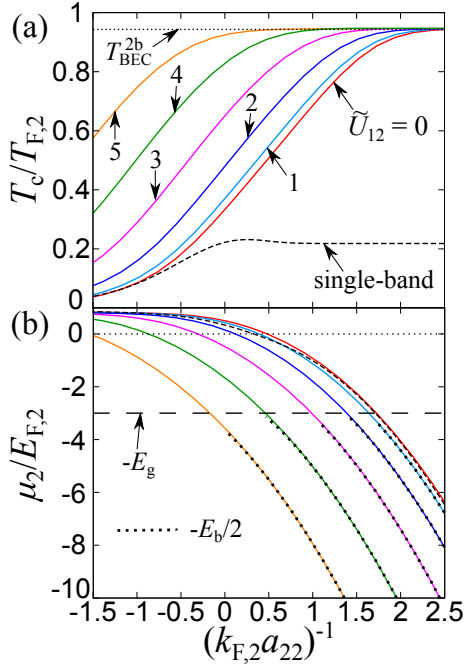


FIG. 3: (a) Critical temperature T_c and (b) chemical potential μ_2 in the hot band vs. $(k_{F,2}a_{22})^{-1}$ at different interband couplings \tilde{U}_{12} (we use the same line-styles in both panels). The constant lines $T_{\text{BEC}}^{2b} = 0.943T_{F,2}$ and $-E_g$, as well as the curves $-E_b/2$ at different \tilde{U}_{12} are also reported for reference.

Here $G_i^0(\mathbf{k}, i\omega_s) = 1/(i\omega_s - \xi_{\mathbf{k},i})$ is the bare Green's function of a i -band particle and $\omega_s = (2s+1)\pi T$ (s integer) is a fermion Matsubara frequency.

The critical temperature T_c is determined by the Thouless criterion⁵⁶, namely the divergence of $\hat{\Gamma}(0,0)$, corresponding to the condition

$$\det [1 + \hat{U}\hat{\Pi}(\mathbf{q}=0, i\nu_l=0)] = 0. \quad (7)$$

This equation needs to be solved together with the particle number equation $n = n_1 + n_2$, where

$$n_i = \sum_{\mathbf{k},\sigma} f(\xi_{\mathbf{k},i}) - T \sum_{\mathbf{q},i\nu_l} \frac{\partial}{\partial \mu_i} \ln \det [1 + \hat{U}\hat{\Pi}(\mathbf{q}, i\nu_l)]. \quad (8)$$

At fixed n , the particle number equation determines the chemical potential μ .

Results – Figure 3 shows the overall critical temperature T_c and the chemical potential $\mu - E_g \equiv \mu_2$ measured from the bottom of the hot band as a function of $(k_{F,2}a_{22})^{-1}$. For vanishing interband interaction, one sees that while in the weak-coupling (BCS) regime T_c and μ_2 essentially coincide with the corresponding single-band results, in the intermediate and strong coupling regions, T_c is greatly enhanced in comparison with the single-band case. In this case the pairing attraction in the hot band drains particles from the cold band, enhancing the critical temperature until, in the strong-coupling limit, the asymptotic value

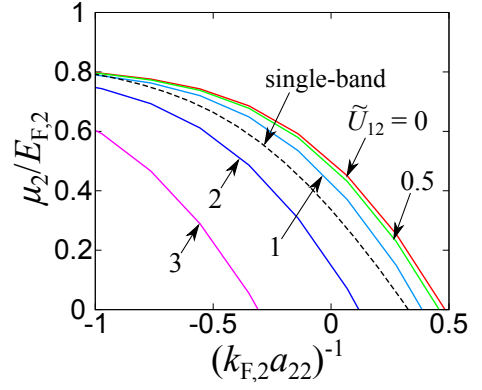


FIG. 4: Chemical potential μ_2 vs. $(k_{F,2}a_{22})^{-1}$ near the unitarity limit $(k_{F,2}a_{22})^{-1} = 0$.

$T_{\text{BEC}}^{2b} = 0.218 (k_{F,t}/k_{F,2})^2 T_{F,2} = 0.943 T_{F,2}$ is reached, corresponding to the condensation temperature for a gas of non-interacting bosons of density $n/2$ and mass $2m$. In this limit, μ_2 coincides with $-E_b/2$, where E_b is the two-body binding energy, which for the decoupled system is given by $E_b = (ma_{22}^2)^{-1}$.

Even more interesting is the situation with a finite interband coupling. In this case the BEC limit can be effectively reached even for rather weak values of the intraband coupling $(k_{F,2}a_{22})^{-1}$. This behavior can be understood by noting that the Thouless criterion (7) can be rewritten as $1 + U_{\text{eff}}\Pi_{22}(0,0) = 0$, where

$$U_{\text{eff}} = U_{22} - U_{12}^2 \Pi_{11}(0,0)/[1 + U_{11}\Pi_{11}(0,0)], \quad (9)$$

is the effective interaction determining T_c . It is the second term in Eq. (9) which leads to a significant increase of the effective pairing interaction when U_{12} increases. It can be shown in particular that in our configuration this term effectively corresponds to a shift $\simeq -0.5k_{F,1}a_{11}\tilde{U}_{12}^2$ of the dimensionless coupling $(k_{F,2}a_{22})^{-1}$ toward stronger couplings.

The effect of the interband coupling can also be seen at the two-body level on the binding energy E_b , which for the coupled system can be obtained from the equation determining the pole of the two-body T -matrix

$$(1 + U_{11}\Pi_{11}^0)(1 + U_{22}\Pi_{22}^0) - U_{12}^2\Pi_{11}^0\Pi_{22}^0 = 0, \quad (10)$$

where Π_{ii}^0 are the vacuum particle-particle bubbles

$$\Pi_{ii}^0 = \frac{mk_0}{2\pi^2} \left[1 - \frac{\sqrt{m|E_i|}}{k_0} \arctan \left(\frac{k_0}{\sqrt{m|E_i|}} \right) \right], \quad (11)$$

and we have defined $E_i = -E_b + 2E_g\delta_{i,1}$ (note that $E_b > 2E_g$ for $U_{12} \neq 0$). One sees in Fig. 3(b) that when \tilde{U}_{12} increases, the binding energy E_b also increases, and μ_2 approaches the BEC limit $-E_b/2$ at progressively weaker intraband couplings $(k_{F,2}a_{22})^{-1}$.

Figure 4 focuses on the behavior of μ_2 near the unitarity limit $(k_{F,2}a_{22})^{-1} = 0$. One can see that in the absence

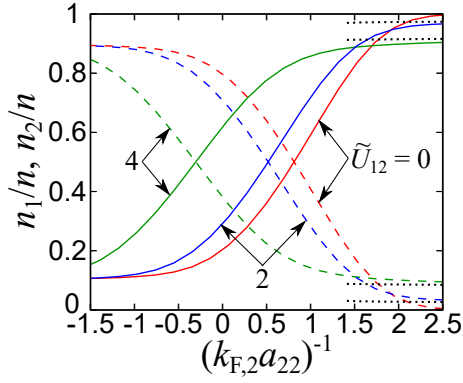


FIG. 5: Number densities n_i (in units of n) in the lower ($i = 1$, dashed line) and upper ($i = 2$, solid line) bands at T_c vs. $(k_{F,2}a_{22})^{-1}$ for different values of \tilde{U}_{12} .

or for weak interband coupling, the chemical potential for the two-band system is larger than for a single-band, such that the crossing of the bottom of the upper band is shifted to larger values of $(k_{F,2}a_{22})^{-1} = 0$. Physically, this is explained by the Pauli-blocking effect due to the occupied states in the cold band which acts to retard the “bosonization” of the Cooper pairs. However, when the interband coupling increases, it overcomes this quantum statistical effect and eventually shifts the bosonization to smaller intraband coupling values.

Figure 5 shows how the fermions distribute between the two bands when the coupling $(k_{F,2}a_{22})^{-1}$ is varied. For different values of the interband coupling \tilde{U}_{12} , one observes in general a progressive transfer of particles from the cold band to the hot one as $(k_{F,2}a_{22})^{-1}$ increases. However, while in the BEC limit one has a full transfer for $\tilde{U}_{12} = 0$, at finite interband coupling the transfer is only partial. This behavior can be understood by solving the two-body bound-state equation $H_{\text{rel}}\Psi = E\Psi$ for the relative motion wave-function $\Psi(r) = (\psi_1(r), \psi_2(r))$, where ψ_1 and ψ_2 are the components in the two bands, H_{rel} is the two-body relative motion Hamiltonian associated with the many-body Hamiltonian (1), and r is the relative distance. In this way one finds that when $\tilde{U}_{12} \neq 0$ the bound-state solution has components in both bands, and the asymptotic value of n_i/n in the BEC limit of the many-body problem coincides with the ratio $||\psi_i||^2/(||\psi_1||^2 + ||\psi_2||^2)$ in the two-body problem (dotted lines in Fig. 5). Here, $||\psi_i||^2 = \int d^3r |\psi_i(r)|^2$; note that the condition $E_b > 2E_g$ is required to have $||\psi_1|| < \infty$.

In this extreme BEC regime, the bosons condensing at T_c are a coherent superposition of two molecular states in the two bands, with wave functions $\psi_i(r) \propto e^{-\sqrt{m|E_i|r}/r}$ and sizes $R_1 = 1/\sqrt{m|2E_g - E_b|}$ and $R_2 = 1/\sqrt{m|E_b|}$. In the less extreme regime whereby the chemical potential μ_2 is between the bottom of the two bands, the two-body bound state is effectively replaced by a quasi-bound state, i.e., a resonance whose energy E_r essentially determines the value of the chemical potential ($\mu_2 \simeq E_r/2$).

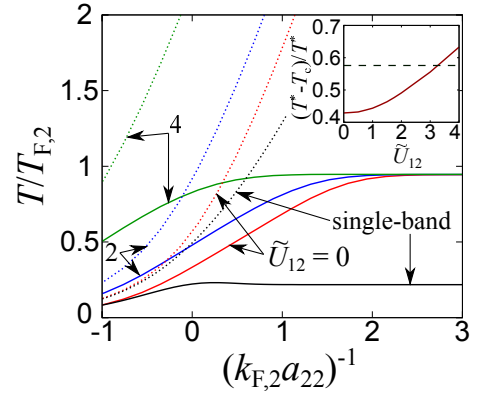


FIG. 6: Critical temperature T_c (solid lines) and pair-breaking temperature T^* (dotted lines) as estimated by the mean-field critical temperature, vs. $(k_{F,2}a_{22})^{-1}$ for different values of \tilde{U}_{12} . The inset shows the ratio $(T^* - T_c)/T^*$ near unitarity [$(k_{F,2}a_{22})^{-1} = 0.07$] as a function of \tilde{U}_{12} . The corresponding value for the single-band case is also reported (dashed line).

The energy E_r corresponds to a peak (narrow for small \tilde{U}_{12}) of the two-body T -matrix, while only the solution of the many-body problem yields the relative distribution of particles between the two bands. Interestingly, unusual vortex configurations with non-triangular geometry, stripes, or multi-quantum-vortex lattices are expected to occur in two-band superconductors with non-equal pair sizes^{41,57} and two-species Bose-Einstein condensates^{58,59}.

In Fig. 6 the preformed pair region of the phase diagram between the mean field temperature T^* and the superfluid critical temperature T_c is investigated for different interband coupling \tilde{U}_{12} . This region is of particular interest because below T^* , pseudogap phenomena and molecular-like pairing are expected to appear, with detectable signatures in the single-particle excitation spectra, depending on the intraband coupling strength^{60,61}. Also, the amount of pair fluctuations in this region is responsible for the detrimental suppression of the superfluid critical temperature. The pairing temperature T^* is strongly enhanced by increasing \tilde{U}_{12} . It is already larger than the corresponding temperature for the single-band case for vanishing interband coupling, because of the larger chemical potential, see Fig. 4. On the other hand, for intraband couplings in the hot band close to unitarity and in a sizable range of $\tilde{U}_{12} \lesssim 3$, the preformed pair region is reduced with respect to the single-band case, as quantified by the temperature window $(T^* - T_c)/T^*$, reported in the inset of Fig. 6. This can be connected with the recent experiment in the multiband FeSe superconductor where BCS-BEC crossover signatures have been confirmed while a pseudogap was not detected⁵³.

In conclusion, we have investigated the BCS-BEC crossover properties for a two-band attractive Fermi system with different strengths of intraband and interband

interactions. For the specific configuration where the intraband coupling is varied from weak to strong in a shallow band coupled to a weakly-interacting deeper band we have found unique features, which are not present in the single-band system, such as a strong amplification of the critical temperature occurring already before unitarity, a significant shrinking of the preformed-pair (pseudogap) region, and the entanglement of two kinds of composite bosons in the BEC regime.

Acknowledgments

H. T. thanks C. A. R. Sá de Melo for useful discussion during the International Conference on

Multi-Condensate Superconductivity and Superfluidity in Solids and Ultra-cold Gases (Multisuper 2018) and acknowledges the hospitality of the Physics Division at the U. of Camerino, where most of this work was done. H. T. was supported by a Grant-in-Aid for JSPS fellows (No.17J03975). This work was supported by the Italian MIUR through the PRIN 2015 program (Contract No. 2015C5SEJJ001) and by the RIKEN iTHEMS program.

-
- ¹ C. A. Regal, M. Greiner, and D. S. Jin, *Observation of Resonance Condensation of Fermionic Atom Pairs*, Phys. Rev. Lett. **92**, 040403 (2004).
 - ² M. Bartenstein, A. Altmeyer, S. Riedl, S. Jochim, C. Chin, J. Hecker Denschlag, and R. Grimm, *Crossover from a Molecular Bose-Einstein Condensate to a Degenerate Fermi Gas*, Phys. Rev. Lett. **92**, 120401 (2004).
 - ³ M. W. Zwierlein, C. A. Stan, C. H. Schunk, S. M. F. Raupach, A. J. Kerman, and W. Ketterle, *Condensation of Pairs of Fermionic Atoms near a Feshbach Resonance*, Phys. Rev. Lett. **92**, 120403 (2004).
 - ⁴ D. M. Eagles, *Possible Pairing without Superconductivity at Low Carrier Concentrations in Bulk and Thin-Film Superconducting Semiconductors*, Phys. Rev. **186**, 456 (1969).
 - ⁵ A. J. Leggett, *Diatomic molecules and Cooper pairs*, in *Modern Trends in the Theory of Condensed Matter*, edited by A. Peralski and R. Przystawa (Springer-Verlag, Berlin 1980).
 - ⁶ P. Nozières and S. Schmitt-Rink, *Bose condensation in an attractive fermion gas: From weak to strong coupling superconductivity* J. Low Temp. Phys. **59**, 195 (1985).
 - ⁷ C. A. R. Sá de Melo, M. Randeria, and J. R. Engelbrecht, *Crossover from BCS to Bose superconductivity: Transition temperature and time-dependent Ginzburg-Landau theory*, Phys. Rev. Lett. **71**, 3202 (1993).
 - ⁸ A. Perali, P. Pieri, G. C. Strinati, and C. Castellani, *Pseudogap and spectral function from superconducting fluctuations to the bosonic limit*, Phys. Rev. B **66**, 024510 (2002).
 - ⁹ Y. Ohashi and A. Griffin, *BCS-BEC crossover in a gas of Fermi atoms with a Feshbach resonance*, Phys. Rev. Lett. **89**, 130402 (2002).
 - ¹⁰ S. Giorgini, L. P. Pitaevskii, and S. Stringari, *Theory of ultracold atomic Fermi gases*, Rev. Mod. Phys. **80**, 1215 (2008).
 - ¹¹ I. Bloch, J. Dalibard, and W. Zwerger, *Many-body physics with ultracold gases*, Rev. Mod. Phys. **80**, 885 (2008).
 - ¹² G. C. Strinati, P. Pieri, G. Röpke, P. Schuck, and M. Urban, *The BCS-BEC crossover: From ultra-cold Fermi gases to nuclear systems*, Phys. Rep. **738**, 1 (2018).
 - ¹³ M. Baldo, U. Lombardo, and P. Schuck, *Deuteron formation in expanding nuclear matter from a strong coupling BCS approach*, Phys. Rev. C **52**, 975 (1995).
 - ¹⁴ H. Stein, A. Schnell, T. Alm, and G. Röpke, *Correlations and pairing in nuclear matter within the Nozières-Schmitt-Rink approach*, Z. Phys. A **351**, 295 (1995).
 - ¹⁵ U. Lombardo, P. Nozières, P. Schuck, H.-J. Schulze, and A. Sedrakian, *Transition from BCS pairing to Bose-Einstein condensation in low-density asymmetric nuclear matter*, Phys. Rev. C **64**, 064314 (2001).
 - ¹⁶ A. Gezerlis and J. Carlson *Strongly paired fermions: Cold atoms and neutron matter* Phys. Rev. C **77**, 032801(R) (2008).
 - ¹⁷ M. Jin, M. Urban, and P. Schuck, *BEC-BCS crossover and the liquid-gas phase transition in hot and dense nuclear matter*, Phys. Rev. C **82**, 024911 (2010).
 - ¹⁸ S. Ramanan and M. Urban, *BEC-BCS crossover in neutron matter with renormalization-group-based effective interaction*, Phys. Rev. C **88**, 054315 (2013).
 - ¹⁹ P. van Wyk, H. Tajima, D. Inotani, A. Ohnishi, and Y. Ohashi, *Superfluid Fermi atomic gas as a quantum simulator for the study of the neutron-star equation of state in the low density region*, Phys. Rev. A **97**, 013601 (2018).
 - ²⁰ R. Micnas, J. Ranninger, and S. Robaszkiewicz, *Superconductivity in narrow-band systems with local nonretarded attractive interactions*, Rev. Mod. Phys. **62**, 113 (1990).
 - ²¹ M. Randeria, N. Trivedi, A. Moreo, and R.T. Scalettar, *Pairing and spin gap in the normal state of short coherence length superconductors*, Phys. Rev. Lett. **69**, 2001 (1992).
 - ²² J. Maly, K. Levin, and D. Z. Liu, *Coulomb correlations and pseudogap effects in a preformed pair model for the cuprates* Phys. Rev. B **54**, R15657(R) (1996).
 - ²³ Y. Tomio, K. Honda, and T. Ogawa, *Excitonic BCS-BEC crossover at finite temperature: Effects of repulsion and electron-hole mass difference*, Phys. Rev. B **73**, 235108 (2006).
 - ²⁴ P. Pieri, D. Neilson, and G. C. Strinati, *Effects of density imbalance on the BCS-BEC crossover in semiconductor electron-hole bilayers*, Phys. Rev. B **75**, 113301 (2007).
 - ²⁵ Y. Chen, A. A. Shanenko, A. Perali, and F. M. Peeters, *Superconducting nanofilms: molecule-like pairing induced by quantum confinement*, J. Phys.: Condens. Matter **24**, 185701 (2012).
 - ²⁶ Y. Lubashevsky, E. Lahoud, K. Chashka, D. Podolsky, and A. Kanigel, *Shallow pockets and very strong coupling superconductivity in FeSe_xTe_{1-x}*, Nat. Phys. **8**, 309 (2012).

- 27 A. Bianconi, *Shape resonances in superstripes*, Nat. Phys. **9**, 536 (2013).
- 28 K. Okazaki, Y. Ito, Y. Ota, Y. Kotani, T. Shimojima, T. Kiss, S. Watanabe, C.-T. Chen, S. Niitaka, T. Hanaguri, H. Takagi, A. Chainani, and S. Shin, *Superconductivity in an electron band just above the Fermi level: possible route to BCS-BEC superconductivity*, Sci. Rep. **4**, 4109 (2014).
- 29 S. Kasahara, T. Watashige, T. Hanaguri, Y. Kohsaka, T. Yamashita, Y. Shimoyama, Y. Mizukami, R. Endo, and H. Ikeda, *Field-induced superconducting phase of FeSe in the BCS-BEC cross-over*, Proc. Natl. Acad. Sci. USA **111**, 16309 (2014).
- 30 S. Conti, A. Perali, F. M. Peeters, and D. Neilson, *Multicomponent Electron-Hole Superfluidity and the BCS-BEC crossover in Double Bilayer Graphene*, Phys. Rev. Lett. **119**, 257002 (2017).
- 31 S. Kasahara, T. Yamashita, A. Shi, R. Kobayashi, Y. Shimoyama, T. Watashige, K. Ishida, T. Terashima, T. Wolf, F. Hardy, C. Meingast, H. v. Löhneysen, A. Levchenko, T. Shibauchi, and Y. Matsuda, *Giant superconducting fluctuations in the compensated semimetal FeSe at the BCS-BEC crossover*, Nat. Commun. **7**, 12843 (2016).
- 32 M. V. Milošević and A. Perali, *Emergent phenomena in multicomponent superconductivity: an introduction to the focus issue*, Supercond. Sci. and Technol. **28**, 060201 (2015).
- 33 D. Innocenti, N. Poccia, A. Ricci, A. Valletta, S. Caprara, A. Perali, A. Bianconi, *Resonant and cross-over phenomena in a multiband superconductor: Tuning the chemical potential near a band edge*, Physical Review B **82**, 184528 (2010).
- 34 K. Hashimoto, K. Cho, T. Shibauchi, S. Kasahara, Y. Mizukami, R. Katsumata, Y. Tsuruhara, T. Terashima, H. Ikeda, M. A. Tanatar, H. Kitano, N. Salovich, R. W. Giannetta, P. Walmsley, A. Carrington, R. Prozorov, and Y. Matsuda, *A Sharp Peak of the Zero-Temperature Penetration Depth at Optimal Composition in $\text{BaFe}_2(\text{As}_{1-x}\text{P}_x)_2$* , Science **336**, 1554 (2012).
- 35 T. Shibauchi, A. Carrington, and Y. Matsuda, *A Quantum Critical Point Lying Beneath the Superconducting Dome in Iron Pnictides*, Annu. Rev. Condens. Matter Phys. **5**, 113 (2014).
- 36 S. Rinott, K. B. Chashka, A. Ribak, E. D. L. Rienks, A. Taleb-Ibrahimi, P. Le Fevre, F. Bertran, M. Randeria and A. Kanigel, *Tuning across the BCS-BEC crossover in the multiband superconductor $\text{Fe}_{1+y}\text{Se}_x\text{Te}_{1-x}$: An angle-resolved photoemission study*, Science Advances **3**, 1602372 (2017).
- 37 A. Perali, A. Bianconi, A. Lanzara, N. L. Saini, *The gap amplification at a shape resonance in a superlattice of quantum stripes: A mechanism for high T_c* , Solid State Commun. **100**, 181 (1996).
- 38 A. Bianconi, A. Valletta, A. Perali, N. L. Saini, *Superconductivity of a striped phase at the atomic limit*, Physica C **296**, 269 (1998).
- 39 A. Guidini and A. Perali, *Band-edge BCS-BEC crossover in a two-band superconductor: physical properties and detection parameters*, Supercond. Sci. and Technol. **27**, 124002 (2014).
- 40 A. V. Chubukov, I. Eremin, and D. V. Efremov, *Superconductivity vs bound state formation in a two-band superconductor with small Fermi energy - applications to Fe-pnictides/chalcogenides and doped SrTiO_3* , Phys. Rev. B **93**, 174516 (2016).
- 41 S. Wolf, A. Vagov, A. A. Shananenko, V. M. Axt, A. Perali, and J. Albino Aguiar, *BCS-BEC crossover induced by a shallow band: Pushing standard superconductivity types apart*, Phys. Rev. B **95**, 094521 (2017).
- 42 L. Salasnich, A. A. Shananenko, A. Vagov, J. Albino Aguiar, and A. Perali, *Screening of pair fluctuations in superconductors with coupled shallow and deep bands: a route to higher temperature superconductivity*, arXiv:1810.03321.
- 43 H. Suhl, B. T. Matthias, and L. R. Walker, *Bardeen-Cooper-Schrieffer Theory of Superconductivity in the Case of Overlapping Bands*, Phys. Rev. Lett. **3**, 552 (1959).
- 44 R. Zhang, Y. Cheng, H. Zhai, and P. Zhang, *Orbital Feshbach Resonance in Alkali-Earth Atoms*, Phys. Rev. Lett. **115**, 135301 (2015).
- 45 G. Pagano, M. Mancini, G. Cappellini, L. Livi, C. Sias, J. Catani, M. Inguscio, and L. Fallani, *Strongly Interacting Gas of Two-Electron Fermions at an Orbital Feshbach Resonance*, Phys. Rev. Lett. **115**, 265301 (2015).
- 46 M. Höfer, L. Riegger, F. Scazza, C. Hofrichter, D. R. Fernandes, M. M. Parish, J. Levinsen, I. Bloch, and S. Fölling, *Observation of an Orbital Interaction-Induced Feshbach Resonance in ^{173}Yb* , Phys. Rev. Lett. **115**, 265302 (2015).
- 47 M. Iskin, *Two-band superfluidity and intrinsic Josephson effect in alkaline-earth-metal Fermi gases across an orbital Feshbach resonance*, Phys. Rev. A **94**, 011604(R) (2016).
- 48 L. He, J. Wang, S.-G. Peng, X.-J. Liu, and H. Hu, *Strongly correlated Fermi superfluid near an orbital Feshbach resonance: Stability, equation of state, and Leggett mode*, Phys. Rev. A **94**, 043624 (2016).
- 49 J. Xu, R. Zhang, Y. Cheng, P. Zhang, R. Qi, and H. Zhai, *Reaching a Fermi-superfluid state near an orbital Feshbach resonance*, Phys. Rev. A **94**, 033609 (2016).
- 50 M. Iskin, *Trapped ^{173}Yb Fermi gas across an orbital Feshbach resonance*, Phys. Rev. A **95**, 013618 (2017).
- 51 P. Zou, L. He, X.-J. Liu, and H. Hu, *Strongly interacting Sarma superfluid near orbital Feshbach resonance*, Phys. Rev. A **97**, 043616 (2018).
- 52 S. Mondal, D. Inotani, and Y. Ohashi, *Single-particle Excitations and Strong Coupling Effects in the BCS-BEC Crossover Regime of a Rare-Earth Fermi Gas with an Orbital Feshbach Resonance*, J. Phys. Soc. Jpn. **87**, 084302 (2018).
- 53 T. Hanaguri, S. Kasahara, J. Böker, I. Eremin, T. Shibauchi, and Y. Matsuda, *Quantum vortex core and missing pseudogap in the multi-band BCS-BEC-crossover superconductor FeSe*, arXiv:1901.09141.
- 54 M. Iskin and C. A. R. Sá de Melo, *BCS-BEC crossover of a collective excitations in two-band superfluids*, Phys. Rev. B **72**, 024512 (2005).
- 55 M. Iskin and C. A. R. Sá de Melo, *Two-band superfluidity from the BCS to the BEC limit*, Phys. Rev. B **74**, 144517 (2006).
- 56 D. J. Thouless, *Perturbation theory in statistical mechanics and the theory of superconductivity*, Ann. Phys. **10**, 553 (1960).
- 57 E. Babaev and M. Speight, *Semi-Meissner state and neither type-I nor type-II superconductivity in multicomponent superconductors*, Phys. Rev. B **72**, 180502(R) (2005).
- 58 E. J. Mueller and Tin-Lun Ho, *Two-Component Bose-Einstein Condensates with a Large Number of Vortices*, Phys. Rev. Lett. **88**, 180403 (2002).
- 59 P. Kuopanportti, J. A. M. Huhtamäki, and M. Möttönen, *Exotic vortex lattices in two-species Bose-Einstein conden-*

- sates, Phys. Rev. A **85**, 043613 (2012).
- ⁶⁰ J. P. Gaebler, J. T. Stewart, T. E. Drake, D. S. Jin, A. Perali, P. Pieri, and G. C. Strinati, *Observation of pseudogap behaviour in a strongly interacting Fermi gas*, Nat. Phys. **6**, 569 (2010).
- ⁶¹ A. Perali, F. Palestini, P. Pieri, G. C. Strinati, J. T. Stewart, J. P. Gaebler, T. E. Drake, and D. S. Jin, *Evolution of the Normal State of a Strongly Interacting Fermi Gas from a Pseudogap Phase to a Molecular Bose Gas*, Phys. Rev. Lett. **106**, 060402 (2011).